Separation Science and Technology
Publication details, including instructions for authors and subscription information:
http://www.informaworld.com/smpp/title~content=t713708471

Adsorption Equilibria of C_8 Aromatic Liquid Mixtures on Y Zeolites Using Headspace Chromatography

Hugo L. B. Buarque[a]; Osvaldo Chiavone-Filho[b]; Célio L. Cavalcante Jr.[a]
[a] Departamento de Engenharia Química Grupo de Pesquisas em Separações por Adsorção—GPSA, Universidade Federal do Ceará, Fortaleza, CE, Brazil [b] Departamento de Engenharia Química, Campus Universitário, Universidade Federal do Rio Grande do Norte, Natal, RN, Brazil

To cite this Article Buarque, Hugo L. B. , Chiavone-Filho, Osvaldo and Cavalcante Jr., Célio L.(2005) 'Adsorption Equilibria of C_8 Aromatic Liquid Mixtures on Y Zeolites Using Headspace Chromatography', Separation Science and Technology, 40: 9, 1817 — 1834

To link to this Article: DOI: 10.1081/SS-200064575

URL: http://dx.doi.org/10.1081/SS-200064575

Separation Science and Technology, 40: 1817–1834, 2005

ISSN 0149-6395 print/1520-5754 online
DOI: 10.1081/SS-200064575

Adsorption Equilibria of C_8 Aromatic Liquid Mixtures on Y Zeolites Using Headspace Chromatography

Hugo L. B. Buarque
Universidade Federal do Ceará, Departamento de Engenharia Química
Grupo de Pesquisas em Separações por Adsorção—GPSA, Campus do
Pici, Fortaleza, CE, Brazil

Osvaldo Chiavone-Filho
Universidade Federal do Rio Grande do Norte, Departamento de
Engenharia Química, Campus Universitário, Natal, RN, Brazil

Célio L. Cavalcante, Jr.
Universidade Federal do Ceará, Departamento de Engenharia Química
Grupo de Pesquisas em Separações por Adsorção—GPSA, Campus do
Pici, Fortaleza, CE, Brazil

Abstract: Liquid phase adsorptive separations are found in several industrial applications such as the recovery of p-xylene from its isomers. In this study, the headspace experimental technique was used to measure pure and multicomponent adsorption equilibria of liquid xylenes in Y zeolite. Data for pure-component equilibrium were determined at temperatures between 80 and 120°C and correlated using the Extended Langmuir model. The parameters for pure components estimated from the correlated data showed good agreement with data reported in previous studies and relatively low deviations when compared to the experimental data dispersion. Using the pure-component data, two models were tested for multicomponent (binary and quaternary) equilibrium correlation: Ideal Adsorbed Solution (IAS) model and Extended Langmuir Multicomponent model. The results from the IAS model did not conform well to the experimental results, indicating the existence of significant nonidealities in the system. The Extended Langmuir model predicted values generally in

Received 23 May 2004, Accepted 31 January 2005

Address correspondence to Célio L. Cavalcante, Jr., On sabbatical at Vanderbilt University, Chem. Eng. Dept., VU Station B 351604, Nashville, TN, USA. Fax: 55-85-288-9601; E-mail: celio@ufc.br

good agreement with the binary and quaternary experimental data measured using the Headspace technique.

Keywords: Xylene isomers, Y zeolite, adsorption equilibrium, headspace technique

INTRODUCTION

Xylene isomers are used as industrial solvents and as intermediates in several synthetic reactions. Therefore these compounds are important starting materials for the petrochemical industries: ethylbenzene is used in the manufacturing of styrene and synthetic polymers; *o*-xylene, *m*-xylene, and *p*-xylene are chemical intermediates in the production of phthalic anhydride, isophthalic acid, and terephthalic acid (polyester and polymer monomer), respectively.

Because of the close boiling points of the C_8 aromatics, their separation has become one of the most important applications of liquid phase adsorption separation processes (1–7). Currently most of the separation of C_8 aromatics is carried out in simulated moving-bed processes at moderate temperatures and pressures with mono or dual-exchanged faujasite zeolites as the adsorbent (7–10). Thus, given its industrial importance, multicomponent adsorption of xylene isomers in the liquid phase must be well described for the purposes of efficient design, scale up, and optimization of adsorptive xylenes separation units. Several studies have reported measurements of adsorption equilibrium of xylenes in Y zeolites in gas and liquid phase (5–7, 10–15) using various traditional techniques, such as batch, thermogravimetry, and chromatographic breakthrough and pulse experiments. The headspace technique, despite having been first used more than 20 years ago, has only recently been reported in the open literature (16).

In this study, pure and multicomponent adsorption equilibrium data of xylenes on a BaY zeolite sample were determined using a headspace chromatographic technique. These data, along with other previously reported data, were used to evaluate multicomponent equilibrium models that may be incorporated into plant simulators for process design.

EXPERIMENTAL

The headspace technique consists of contacting a given liquid volume with a given adsorbent mass in sealed vials (equilibrium cells). After a sufficient amount of time is allowed, there will be three equilibrated phases: vapor, liquid, and adsorbed. The vapor phase is sampled and, from its composition, we may use a proper VLE (Vapor-Liquid Equilibrium) relationship to calculate the composition of the liquid phase. The adsorbed-phase concentration may then be determined by a simple mass balance. Figure 1 illustrates the experimental setup of the technique. More details about the experimental procedures may be found elsewhere (16, 17).

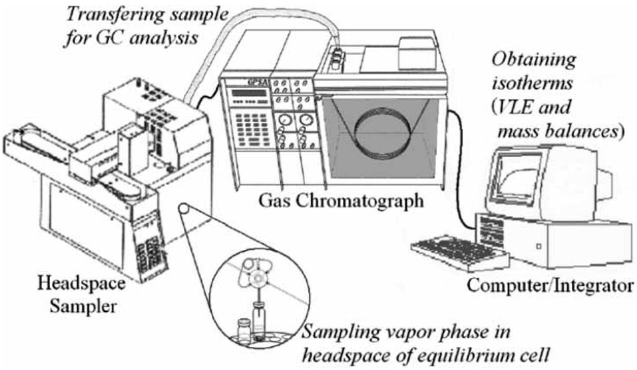

Figure 1. Schematic setup of headspace technique.

C_8 aromatic isomers (Fig. 2) and decane (as inert) with purity higher than 99% wt were used in the experiments. The adsorbent, in the form of spherical pellets (Fig. 3), is a BaY zeolite with physical and chemical parameters shown in Table 1. Prior to use in the experiments, the adsorbent was treated with dry nitrogen at a flow rate of 20 mL/g/min in a cylindrical electrical oven. Initially, the sample was maintained at 100°C for 1 h and then heated slowly at approximately 100°C/h up to 180°C. It was then held at the final temperature for at least 2 h to reduce ambient adsorbed water from the adsorbent to about 3% wt. This humidity is desired to obtain the optimal para-selectivity of Y zeolites in xylene systems (3, 10, 18). After that, the adsorbent particles were allowed to cool down to room temperature, still under nitrogen flow, and then immediately used in the equilibrium cells.

The experimental setup had a Hewlett-Packard Headspace Sampler (HP-7694) connected to a Hewlett-Packard Gas Chromatograph (HP-5890). Their operational parameters are shown in Tables 2 and 3. A thermostatic bath was also used to preheat the equilibrium cells to attain approximate equilibrium conditions, reducing the equilibrium time into the heater of the headspace sampler.

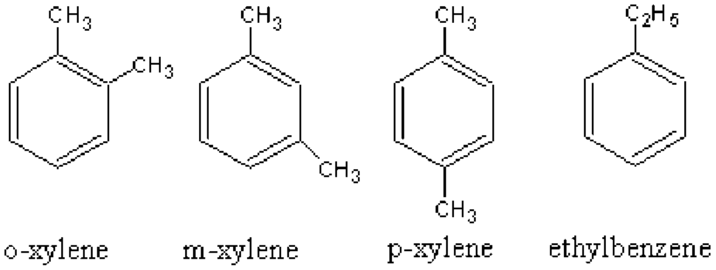

Figure 2. C_8 aromatic isomers.

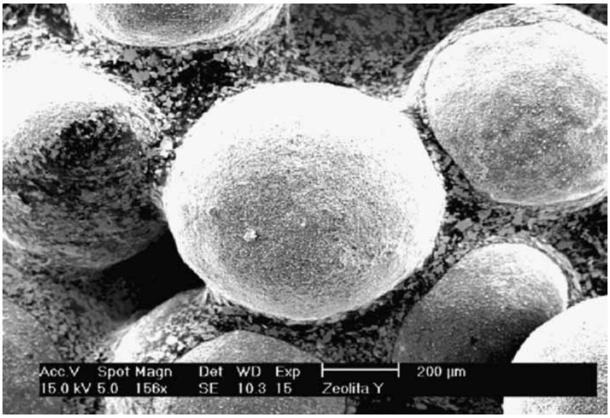

Figure 3. SEM micrograph of the adsorbent.

EQUILIBRIUM MODELS

Langmuir (19) and Dual-Site Langmuir (20) equilibrium models were used to evaluate the pure-component experimental data. The Langmuir equation, Eq. (1), has only two parameters and usually provides a tractable and satisfactory representation of the equilibrium for use in the simulation of industrial units. The Dual-Site Langmuir equation - DSL Eq. (2), a two site heterogeneous surface model, should correlate experimental data better, given the higher number of parameters, and may be more adequate when two-parameter-only equations do not fit the adsorption isotherm data accurately.

$$q = \frac{q_m b C}{1 + bC} \tag{1}$$

$$q = \frac{q_{m,A} b_A C}{1 + b_A C} + \frac{q_{m,B} b_B C}{1 + b_B C} \tag{2}$$

Table 1. Adsorbent properties

Macro and mesopore volume	$0.253\,\mathrm{cm^3/g}$
Solid density	$2.945\,\mathrm{g/cm^3}$
Bulk density	$1.390\,\mathrm{g/cm^3}$
Macropores void fraction	0.3517
Micropores void fraction	0.1762
Solid void fraction	0.4721
Average pellet diameter	600 µm
Crystal diameter	1–3 µm
Water uptake at 25°C	~25%wt

Table 2. Headspace sampler setup

Vial volume	22 mL
Vial equilibrium time	50 min
Vial temperature	80/100/120°C
Loop temperature	90/110/130°C
Transfer line temperature	100/120/140°C
Carrier gas pressure	9.3 to 10.0 psig
Vial pressure	4.8 to 5.0 psig
Pressurization time	0.20 min
Loop fill time	0.16 min
Loop equilibrium time	0.01 min
Inject time	0.50 min
Shake	0 = Off
GC cycle time	10 min

In these equations, q and C are adsorbed- and fluid-phase concentrations; q_m and b are model parameters. The subscripts A and B refer to heterogeneous patches on the solid surface.

For multicomponent equilibrium (binary and quaternary), two models were tested to correlate our data: Ideal Adsorbed Solution (IAS) model and Extended Langmuir Multicomponent model.

The Ideal Adsorbed Solution (IAS) Theory, proposed by Myers and Prausnitz (21), can be used to predict multicomponent equilibria directly from pure-component isotherms and may be considered as analogous to Vapor-Liquid Equilibria Raoult's Law. It assumes that the adsorbent is inert and that equilibrium is attained at constant temperature and surface potential. There are interactions between adsorbed molecules but the molecules cannot distinguish the difference between the various components present in the mixture. Equilibrium can be estimated from Eqs. (3) and (4).

$$x_i C = w_i C_i^o(T, \pi) \tag{3}$$

$$q = \frac{1}{\sum_i w_i / q_i^o(C_i^o)} \tag{4}$$

Table 3. Gas chromatograph setup

Column	Carbowax 50 m × 0.25 mm, df = 0.2 μm
Oven temperature	Isothermal at 70°C
Carrier gas	H_2, 10 psi
Injector	Headspace and Splitter, 260°C 80 mL/min + 40 mL/min
Detector	FID, 280°C, range 6 makeup (N_2), 30 mL/min H_2/Air, 30/400 mL/min
Run time	300 min

In these equations, x_i and w_i are mole fractions of component i in liquid and adsorbed phase; q and C are adsorbed-phase and fluid-phase total concentrations; C_i^o is the pure-component fluid phase concentration at equilibrium at the same temperature T and spreading pressure π; and q_i^o is the pure component adsorbed phase concentration at C_i^o and temperature T.

The Extended Langmuir multicomponent model, as adopted by Talu and Hayhurst (22) and Mathias et al. (23), was used to correlate pure-component and binary data simultaneously in order to find an optimal set of parameters for each component [Eq. (5)]. This model includes an exponential vant'Hoff temperature-dependent term to allow data correlation at different temperatures.

$$q_i = \frac{q_{m,i} b_{o,i} C_i EXP(-Q_i/RT)}{1 + \sum_j q_{m,j} b_{o,j} C_j EXP(-Q_j/RT)} \tag{5}$$

In Eq. (5), q_m, b_o, and Q are model parameters; the subscripts i and j refer to components of the mixture. For calculation purposes, the Extended Langmuir model provides an adequate and numerically convenient way to predict multicomponent equilibria when pure component equilibrium has been well determined. Such a model requires that all the components have the same saturation capacity for thermodynamic consistency.

RESULTS AND DISCUSSION

Experimental Results for Pure and Multicomponent Equilibria

The pure-component liquid phase adsorption data obtained in this study are presented in Fig. 4. The experiments were performed in a wide concentration range and at temperatures between 80–120°C. The measured isotherms had the type I shape of IUPAC classification (24).

Table 4 shows the data for the binary system *p*-xylene/*m*-xylene on BaY zeolite at temperatures between 80–120°C. Quaternary equilibrium data are presented in Table 5. Raoult's Law was assumed valid for Vapor-Liquid Equilibria of the xylene isomers. This was used to estimate the liquid phase composition from the vapor phase composition measurements from the Headspace Chromatography. Pure component vapor pressure data were calculated using the DIPPR data compilation (25).

In all experiments, we observed that a liquid/solid ratio of about 13% wt was achieved for the saturation of the zeolite with C_8 aromatics, as shown in Fig. 5.

Table 6 presents the selectivities calculated from experimental multicomponent data of this study, with values at the same order of magnitude of similar previous reports (7, 14, 26). As expected, the selectivities of *p*-xylene with respect to *m*-xylene, *o*-xylene, and ethylbenzene are always much greater than one.

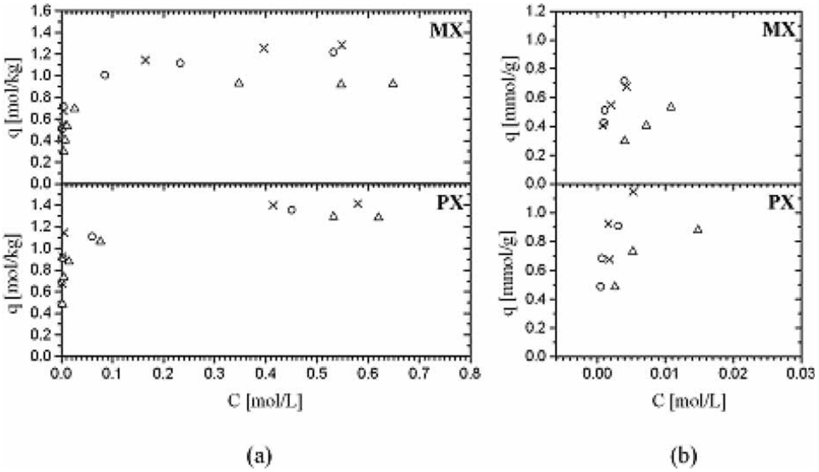

Figure 4. Adsorption isotherms of *m*-xylene and *p*-xylene on BaY zeolite: (a) entire concentration range; (b) low concentration range. Symbols: (○) 80°C; (X) 100°C; (△) 120°C.

The selectivities between *p*-xylene and the other C_8 isomers decrease almost linearly with increasing temperature (in the conditions that were studied), as shown in Fig. 6. Also, at a given temperature, we may observe a strong dependency of selectivity with liquid phase concentration (Fig. 7). The same behavior has been previously reported for similar systems using different experimental procedures (7, 11). The strong dependency of the selectivity with the composition of the mixture suggests nonideality of the adsorbed phase. So models based on adsorbed phase ideality will probably not be able to adequately predict multicomponent equilibria directly from pure-component adsorption data (11), as will be seen in the next section.

Table 4. Binary equilibrium data of adsorption of *p*-xylene/*m*-xylene on Y zeolite

T [°C]	q [mol/kg]	W_{PX}	C [mol/L]	X_{PX}
	1.225	0.101	7.654	0.030
80	1.254	0.500	7.648	0.196
	1.240	0.900	7.629	0.709
	1.430	0.101	7.481	0.032
100	1.388	0.500	7.474	0.205
	1.310	0.900	7.456	0.702
	1.113	0.101	7.302	0.035
120	1.252	0.501	7.294	0.231
	1.274	0.898	7.276	0.707

Table 5. Quaternary equilibrium data of adsorption of C_8 aromatics on Y zeolite

T [°C]	80	100	120
q [mol/kg]	1.301	1.308	1.191
w_{PX}	0.248	0.248	0.250
w_{MX}	0.250	0.250	0.250
w_{OX}	0.250	0.250	0.250
w_{EB}	0.252	0.252	0.250
C [mol/L]	7.720	7.544	7.363
x_{PX}	0.081	0.088	0.101
x_{MX}	0.317	0.316	0.326
x_{OX}	0.413	0.387	0.371
x_{EB}	0.189	0.209	0.202

Modeling of Adsorption Equilibria

For the modeling procedure, we used the pure and multicomponent data obtained in this study plus pure-component data previously reported for the same adsorbent using different experimental methods (27, 28). We had an overall total of 232 pure and multicomponent data points. Figure 8 shows

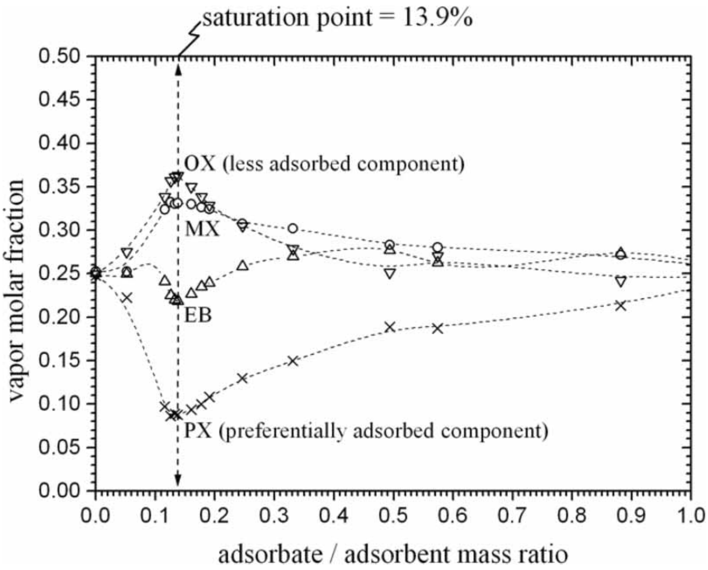

Figure 5. Multicomponent experimental run: C_8 aromatic mixture in BaY zeolite at 80°C.

Table 6. Experimental selectivities of C$_8$ aromatics on Y zeolite at different temperatures

T [°C]	X_{PX}	X_{MX}	X_{OX}	W_{PX}	W_{MX}	W_{OX}	$\alpha_{PX\text{-}MX}$	$\alpha_{PX\text{-}OX}$	$\alpha_{PX\text{-}EB}$
80	0.030	0.970	—	0.101	0.899	—	3.65	—	—
	0.196	0.804	—	0.500	0.500	—	4.11	—	—
	0.709	0.291	—	0.900	0.100	—	3.69	—	—
	0.081	0.317	0.413	0.248	0.250	0.250	3.87	5.06	2.29
100	0.032	0.968	—	0.101	0.899	—	3.42	—	—
	0.205	0.795	—	0.500	0.500	—	3.88	—	—
	0.702	0.298	—	0.900	0.100	—	3.82	—	—
	0.088	0.316	0.387	0.248	0.250	0.250	3.55	4.37	2.34
120	0.035	0.965	—	0.101	0.899	—	3.05	—	—
	0.231	0.769	—	0.5016	0.499	—	3.34	—	—
	0.707	0.293	—	0.898	0.102	—	3.64	—	—
	0.101	0.326	0.371	0.250	0.250	0.250	3.22	3.67	1.98

an example of the pure-component data that were used, in this case for *p*-xylene.

Initially, a nonlinear regression was performed using the pure-component data to verify the adequacy of both the Langmuir (L) and Dual-Site Langmuir (DSL) models for the system studied. The DSL model fit the data somewhat

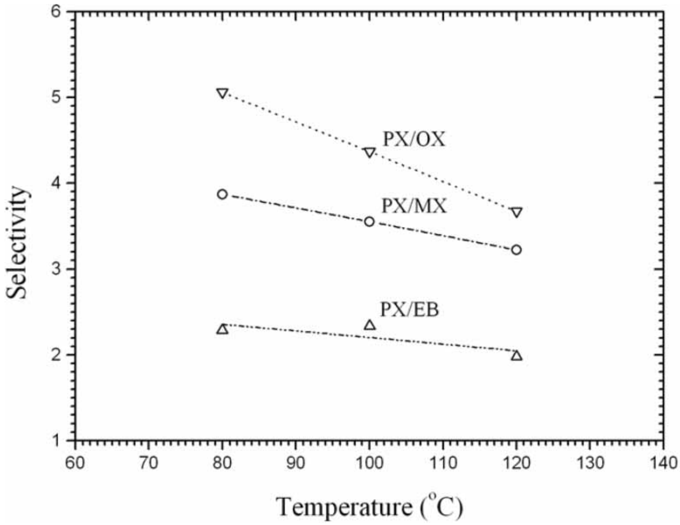

Figure 6. Temperature dependence of C8 isomers selectivities in BaY zeolite at $X_{PX} = 0.081$ (quaternary equilibrium data).

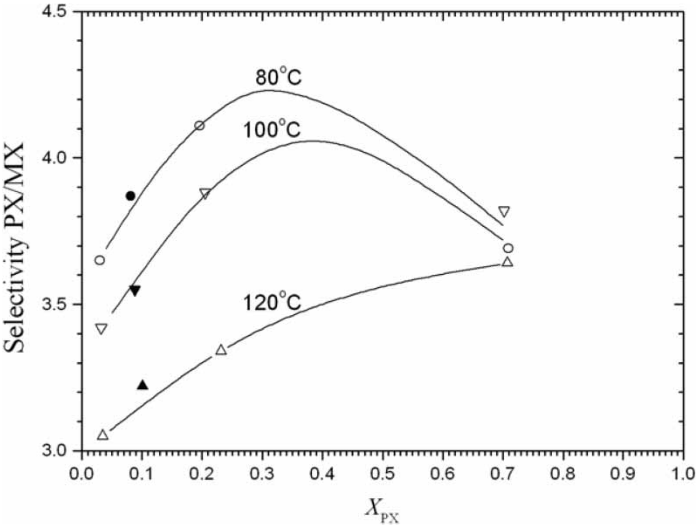

Figure 7. PX/MX selectivity vs. *p*-xylene composition in the liquid phase (open symbols: binary data; solid symbols: quaternary data).

better than the Langmuir model, but both had average relative errors of less than 10% as shown in Table 7.

To evaluate the necessity of using the more complex DSL model instead of the simpler Langmuir model, we have used the parameter Heterogeneity Degree (Ψ), as proposed by Mathias et al. (23) and defined in Eq. (6). This

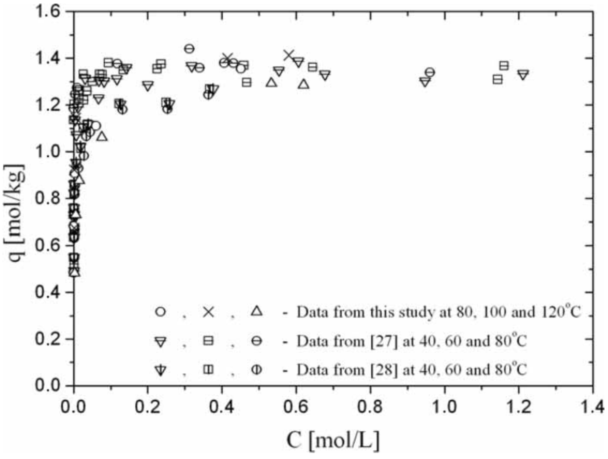

Figure 8. Pure-component isotherms of *p*-xylene on BaY zeolite used in the modeling study.

Table 7. Average relative errors (%) obtained from the Langmuir (L) and Double-Site Langmuir (DSL) models for pure-component equilibrium (no pure-component data available for *o*-xylene)

	Data from this study			Data from Cavalcante and Gubulin (27)			Data from Neves (28)		
	80°C	100°C	120°C	40°C	60°C	80°C	40°C	60°C	80°C
PX–L	8.7	7.8	6.7	4.8	9.4	2.6	7.4	7.9	7.3
PX–DSL	4.0	9.9	2.6	4.6	8.1	1.2	5.2	5.6	5.6
MX–L	7.1	9.5	1.9	1.2	1.8	4.1	n.a.	n.a.	n.a.
MX–DSL	1.9	0.9	3.2	0.2	2.2	2.2	n.a.	n.a.	n.a.
EB–L	n.a.	n.a.	n.a.	n.a.	n.a.	n.a.	5.4	4.4	3.3
EB–DSL	n.a.	n.a.	n.a.	n.a.	n.a.	n.a.	1.4	1.9	0.8

n.a.—data not available.

parameter, derived from energy distributions in terms of their central moments, is defined as the ratio of the standard deviation to the mean of the standard distribution (29). Table 8 shows the calculated values of Ψ, indicating that the heterogeneity of the system is negligible in the conditions of our study (average values less than unity) (23, 29, 30). Therefore we should not strictly need to use the more complex DSL model to better represent our pure-component data.

$$\Psi = \left[\frac{(1 + q_{m,B}/q_{m,A})(1 + b_B^2 q_{m,B}/b_A^2 q_{m,A})}{(1 + b_B q_{m,B}/b_A q_{m,A})^2} - 1\right]^{1/2} \tag{6}$$

So we have used the simple pure-component Langmuir model with a third parameter (Q/R) to account for temperature variations [Eq. (7)] for the

Table 8. Heterogeneity degree parameter (Ψ) calculated from the DSL model

	Ψ								
	Data from this study			Data from Cavalcante and Gubulin (27)			Data from Neves (28)		
	80°C	100°C	120°C	40°C	60°C	80°C	40°C	60°C	80°C
p-xylene	0.8	0.7	0.7	0.6	0.6	0.7	0.1	0.2	0.1
m-xylene	0.7	0.9	0.0	0.1	0.1	0.2	n.a.	n.a.	n.a.
ethylbenzene	n.a.	n.a.	n.a.	n.a.	n.a.	n.a.	1.2	1.3	1.8

n.a.—experimental data is not available.

Table 9. Langmuir parameters obtained from the pure-component experimental data (no pure-component data available for *o*-xylene)

C_8 aromatic	q_m [mmol/g]	b [L/mol]	Q/R [K]	δ (%)
p-xylene	1.208	0.498	−2666.3	10.6
m-xylene	1.208	12.583	−1296.5	9.8
ethylbenzene	1.208	0.013	−3474.7	5.4

building of a predictive model of multicomponent equilibrium. We correlated simultaneously all C_8 aromatics isotherms at several temperatures. Identical maximum sorption capacities were obtained for the xylene isomers on the zeolite. Table 9 shows the parameters that were obtained with the Langmuir model as well as the average deviation for each system.

$$q = \frac{q_m bC\,exp\,(-Q/RT)}{1 + bC\,exp\,(-Q/RT)} \tag{7}$$

Using these Langmuir parameters, we predicted the binary data of *p*-xylene/*m*-xylene and *p*-xylene/ethylbenzene by applying the IAS model. In Table 10, we see that the average relative errors obtained with these predictions are very high (generally greater than 20%), indicating that the IAS model did not represent well the C_8 aromatics/Y zeolite multicomponent behavior. These results can be attributed either to the nonideality of the adsorbed phase (as seen from the selectivity results) or to lack of appropriate accuracy of our pure-component data at low concentrations (31–33).

We then decided to use the Langmuir Extended model (Eq. 5) by fitting, in a unique regression, all pure-component and binary data, as done in previous studies (22,23). The parameters thus obtained are shown in Table 11. Using these parameters, we recalculated all of our pure-component and binary data, yielding average errors as shown in Table 12. It may be

Table 10. Average relative deviations obtained with the IAS model for *p*-xylene binary mixtures with *m*-xylene (PX/MX) and with ethylbenzene (PX/EB)

System	*T* (°C)	δ_{PX} (%)	δ_{MX} (%)	δ_{EB} (%)
PX/MX[a]	120	39.2	60.0	
	100	43.1	44.2	
	80	31.8	48.2	
	60	26.8	43.8	
PX/EB[a]	80	19.7		20.6
	60	12.3		13.1

[a] data from Neves (28) and this study.

Table 11. Langmuir parameters for xylenes on Y zeolite fitted from pure-component and binary experimental data

C_8 aromatics	q_m [mol/kg]	b_o [L/mol]	Q/R [K]
p-xylene	1.193	0.324	−2825.9
m-xylene	1.193	0.209	−2473.4
o-xylene	1.193	1.080	−1732.1
ethylbenzene	1.195	0.216	−2628.1

observed that, despite relatively large errors for the pure-component data, the errors for the binary data are generally less than 10%. Figures 9–11 present the *w*-*x* binary diagrams, showing the good conformity of the experimental data to the proposed model. For comparison, we also show the IAS predictions calculated using a Langmuir isotherm for the pure-component data.

Using the same parameters, we have estimated the quaternary equilibrium data, as shown in Table 13. It is observed that, except for *o*-xylene (for which we had only few data available), our estimates are in general good agreement with the experimental values.

CONCLUSIONS

The headspace technique was used to obtain pure, binary, and quaternary equilibrium experimental data for the adsorption of xylene isomers on a BaY zeolite. Langmuir and Dual-Site Langmuir models were used to evaluate the pure-component experimental data obtained. It was observed that, within the conditions that were tested, it is unnecessary to use a more complex model (DSL) to represent the equilibrium behavior of this system.

The correlation of the multicomponent data from the pure-component data was attempted using the Ideal Adsorbed Solution (IAS) model. However, these predictions were not satisfactory, yielding large average

Table 12. Average relative deviations obtained with Extended Langmuir model (pure-component and binary data)

System	δ_{PX} (%)	δ_{MX} (%)	δ_{OX} (%)	δ_{EB} (%)
PX	10.8	—	—	—
MX	25.8	—	—	—
EB	5.8	—	—	—
PX/MX	5.7	6.6	—	—
PX/OX	4.9	—	5.1	—
PX/EB	4.7	—	—	3.3

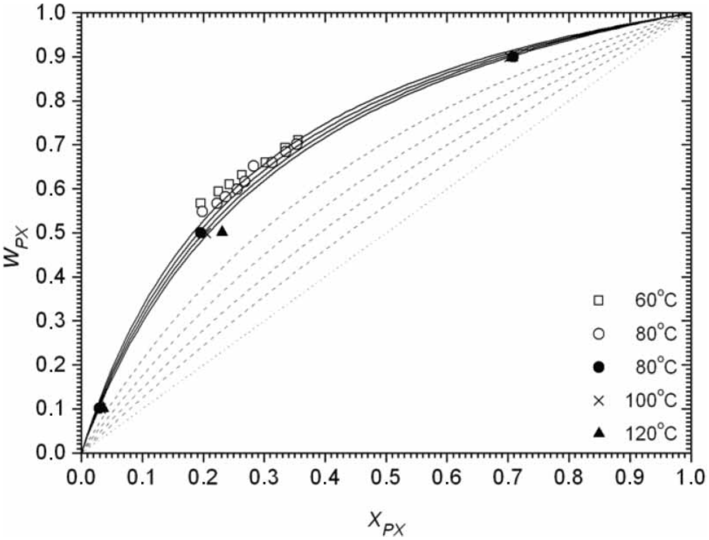

Figure 9. Binary Data PX/MX. Solid symbols are experimental data from this study; open symbols are experimental data from Neves (28); solid lines are multicomponent Langmuir fittings; dashed lines are IAS predictions.

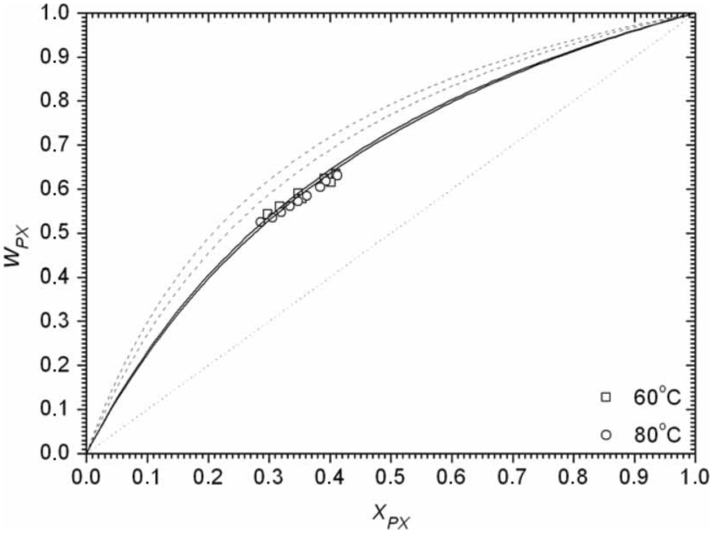

Figure 10. Binary Data PX/EB. Symbols are experimental data from Neves (28); solid lines are multicomponent Langmuir fittings; dashed lines are IAS predictions.

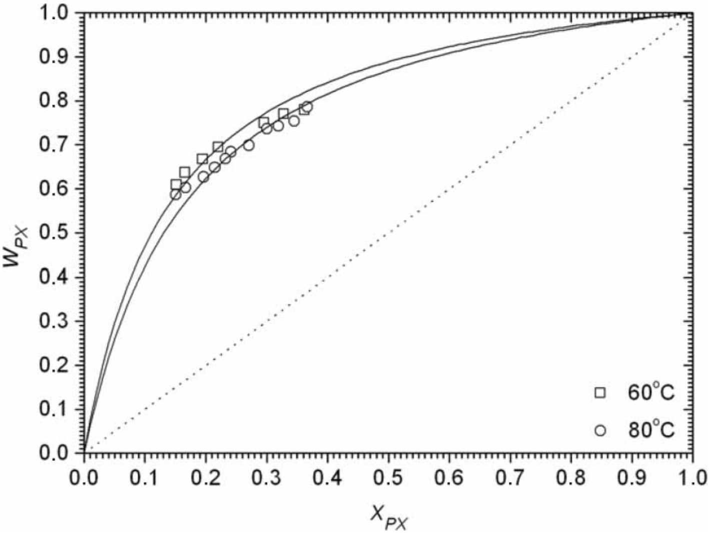

Figure 11. Binary Data PX/OX. Symbols are experimental data from Neves (28); solid lines are multicomponent Langmuir fittings.

errors between prediction and experimental observation, which was attributed either to the nonideality of the adsorbed phase or to low accuracy of our pure-component data at the Henry's law region.

The use of an Extended Langmuir model provided better agreement with the experimental equilibrium data for C_8 aromatics on Y zeolite, showing

Table 13. Quaternary data estimates using the Extended Langmuir model ($X =$ liquid phase composition; $W_{EXP} =$ Experimental solid phase composition; $W_{ELM} =$ solid phase composition estimated using the Extended Langmuir model)

T(°C)		PX	MX	OX	EB
80	X	0.081	0.317	0.413	0.189
	W_{EXP}	0.248	0.250	0.250	0.252
	W_{ELM}	0.235	0.260	0.276	0.229
100	X	0.088	0.316	0.387	0.209
	W_{EXP}	0.248	0.250	0.250	0.252
	W_{ELM}	0.238	0.242	0.282	0.238
120	X	0.101	0.326	0.371	0.202
	W_{EXP}	0.250	0.250	0.250	0.250
	W_{ELM}	0.260	0.238	0.227	0.275
Average error, δ (%)		4.4	6.0	10.8	8.2

average deviations generally less than 10%, even for quartenary equilibrium. In this way, an easy and simplified way of representing equilibrium data for simulation purposes could be proposed and satisfactorily used.

NOMENCLATURE

VLE	vapor-liquid equilibrium
DSL	dual-site Langmuir model
IAS	ideal adsorbed solution model
EB	ethylbenzene
MX	*m*-xylene
OX	*o*-xylene
PX	*p*-xylene
C	liquid phase concentration, mol/m^3
b	isotherm parameter
Q	isotherm parameter
q	adsorbed phase concentration, mol/kg
q_m	maximum coverage in Langmuir isotherm, mol/kg
R	gas constant
T	temperature, K
w	mole fraction in adsorbed phase
x	mole fraction in liquid phase

Greek Symbols

α	selectivity
δ	average relative error, %
Ψ	heterogeneity degree (eq. 6)
π	spreading Pressure

Subscripts

A, B	heterogeneous patches on the solid
i, j	components of the mixture
o	standard state

ACKNOWLEDGMENTS

The authors acknowledge financial support from CNPq and COPENE.

REFERENCES

1. Stine, L.O., Broughton, D.B. Process for the Production and Recovery of Ortho-Xylene, Para-Xylene and Ethylbenzene. US Patent 3,636,121, November 7, 1969; to UOP.

2. Broughton, D.B., Neuzil, R.W., Pharis, J.M., and Brearly, C.S. (1970) The parex process for recovering paraxylene. *Chem. Engng. Prog.*, 66 (9): 70–75.
3. Neuzil, R.W. (1975) Process for Separating Para-Xylene. US Patent 3,997,620, October 28; to UOP.
4. Yan, T.Y. (1988) Effects of moisture in separation of C_8 aromatics using medium-pore zeolites. *Ind. Eng. Chem. Res.*, 27 (9): 1665–1668.
5. Li, M.H., Hsiao, H.C., and Yih, S.M. (1991) Adsorption equilibria of xylene isomers on a KBa-Y zeolite. *J. Chem. Eng. Data*, 36 (2): 244–248.
6. Hulme, R., Rosensweig, R.E., and Ruthven, D.M. (1991) Binary and ternary equilibria for C_8 aromatics on K-Y faujasite. *Ind. Eng. Chem. Res.*, 30 (4): 752–760.
7. Tournier, H., Barreau, A., Tavitian, B., Le Roux, D., Moïse, J.C., Bellat, J.P., and Paulin, C. (2001) Adsorption equilibrium of xylene isomers and *p*-diethylbenzene on a prehydrated BaX zeolite. *Ind. Eng. Chem. Res.*, 40 (25): 5983–5990.
8. Minceva, M. and Rodrigues, A.E. (2002) Modeling and simulation moving bed for the separation of *p*-xylene. *Ind. Eng. Chem. Res.*, 41 (14): 3454–3461.
9. Minceva, M. and Rodrigues, A.E. (2003) Influence of the transfer line dead volume on the performance of an industrial scale simulated moving bed for *p*-xylene separation. *Separ. Sci. Technnol.*, 38 (7): 1463–1497.
10. Bellat, J.P., Moïse, J.C., Cottier, V., Paulin, C., and Methivier, A. (1998) Effect of water content on the selective coadsorption of gaseous *p*-xylene and *m*-xylene on the BaY zeolite. *Sep. Sci. Technol.*, 33 (15): 2335–2348.
11. Cottier, V., Bellat, J.P., Simonot-Grange, M.H., and Methivier, A. (1997) Adsorption of *p*-xylene/*m*-xylene gas mixtures on BaY and NaY zeolites. Coadsorption equilibria and selectivities. *J. Phys. Chem. B*, 101 (24): 4798–4802.
12. Methvier, A. (1998) Influence of oxygenated contaminants on the separation of C_8 aromatics by adsorption on faujasite zeolites. *Ind. Eng. Chem. Res.*, 37 (2): 604–608.
13. Santacesaria, E., Morbidelli, M., Danise, P., Mercenari, M., and Carrà, S. (1982) Separation of xylenes on Y zeolites. 1. Determination of the adsorption equilibrium parameters, selectivities, and mass transfer coefficients through finite bath experiments. *Ind. Eng. Chem. Process Des. Dev.*, 21 (3): 440–457.
14. Tournier, H., Barreau, A., Tavitian, B., Le Roux, D., Sulzer, C., and Beaumont, V. (2000) Two experimental methods to study adsorption equilibria of xylene isomers in the liquid phase on a Y zeolite. *Microporous Mesoporous Mater.*, 39: 537–547.
15. Minceva, M. and Rodrigues, A.E. (2004) Adsorption of xylenes on faujasite-type zeolite: equilibrium and kinetics in batch adsorber. *Chemical Engineering Research and Design*, 82 (A5): 667–681.
16. Torres, A.E.B., Neves, S.B., Abreu, J.C.N., Cavalcante, C.L., Jr., and Ruthven, D.M. (2001) Single- and Multi-Component Liquid Phase Adsorption Measurements by Headspace Chromatography. *Braz. J. Chem. Eng.*, 18 (1): 121–125.
17. Buarque, H.L.B. (1999) *Adsorção Multicomponente de Xilenos em Zeólita Y no Equilíbrio*; Master's Thesis; UFRN: Natal, Brazil.
18. Furlan, L.T., Chaves, B.C., and Santana, C.C. (1992) Separation of liquid-mixtures of paraxylene and orthoxylene in X-zeolites - the role of water-content on the adsorbent selectivity. *Ind. Eng. Chem. Res.*, 31 (7): 1780–1784.
19. Langmuir, I. (1918) The adsorption of gases on plane surfaces of glass, mica and platinum. *J. Am. Chem. Soc.*, 40 (9): 1361–1403.
20. Myers, A.L. (1983) Activity coefficients of mixtures adsorbed on heterogeneous surfaces. *AIChE J.*, 29 (4): 691–693.

21. Myers, A.L. and Prausnitz, J.M. (1965) Thermodynamics of mixed-gas adsorption. *AIChE J.*, 11 (1): 121–127.
22. Talu, O. and Hayhurst, D.T. (1989) Isosteric Heat of Adsorption by the Virial Isotherm Equation. *AIChE Annual Meeting*, San Francisco, CA, November.
23. Mathias, P.M., Kumar, R., Moyer, J.D., Jr., Schork, J.M., Srinivasan, S.R., Auvil, S.R., and Talu, O. (1996) Correlation of multicomponent gas adsorption by the dual-site langmuir model. Application to nitrogen/oxygen adsorption on 5A-zeolite. *Ind. Eng. Chem. Res.*, 35 (7): 2477–2483.
24. Sing, K.S.W., Everett, D.H., Haul, R.A.W., Moscou, L., Pierotti, R.A., Rouquerol, J., and Siemieniewska, T. (1985) Reporting physisorption data for gas/solid systems with special reference to the determination of surface area and porosity. *Pure Appl. Chem.*, 57: 603–619.
25. Daubert, T.E. and Danner, R.P. (1995) *DIPPR Data Compilation, Version 13.0*, AIChE: New York.
26. Moya-Korchi, V., Tavitian, B., and Méthivier, A. (1996) Thermodynamics of adsorption of C8 aromatics solutions on Y zeolites. In *Fundamentals of Adsorption*, Proceedings of the Fifth International Conference on Fundamentals of Adsorption, Asilomar, USA, 1995; LeVan, M.D., ed.; Kluwer Academic Publishers: Boston, MA, 651–658.
27. Cavalcante, C.L., Jr. and Gubulin, J.C. (1990) Liquid phase selective adsorption of xylenes. *I. Chem. E. Symp. Series*, 118: 83–94.
28. Neves, S.B. (1995) *Adsorção Líquido-Sólido. Estudo Experimental e Modelagem de uma Coluna de Leito Fixo*; Master's Thesis; UFBA: Salvador, Brazil.
29. Sircar, S. (1991) Role of adsorbent heterogeneity on mixed gas adsorption. *Ind. Eng. Chem. Res.*, 30: 1032.
30. Sircar, S. and Myers, A.L. (1984) Energy distributions for equilibrium adsorption of gases on heterogeneous surfaces. *AIChE Symp. Series.*, 80: 55–61.
31. Yu, J.W. and Neretnieks, I. (1990) Single-component and multicomponent adsorption equilibria on activated carbon of methylcyclohexane, toluene, and isobutyl methyl ketone. *Ind. Eng. Chem. Res.*, 29: 220–231.
32. Sircar, S. (1995) Influence of adsorbate size and adsorbent heterogeneity on IAST. *AIChE J.*, 41 (5): 1135–1145.
33. Talu, O. (1998) Needs, status, techniques and problems with binary gas adsorption experiments. *Adv. Colloid. Interface Science*, 76–77: 227–269.